Direct Measurement of Polysulfide Shuttle Current: A Window into Understanding the Performance of Lithium-Sulfur Cells

Direct Measurement of Polysulfide Shuttle Current: A Window into Understanding the Performance of Lithium-Sulfur Cells

Derek Moy,[a] A. Manivannan,[b,*] and S. R. Narayanan[a,,z]**

[a]*Loker Hydrocarbon Research Institute, Department of Chemistry, University of Southern California, Los Angeles, California 90089, USA*
[b]*US Department of Energy, National Energy Technology Laboratory, Morgantown, West Virginia 26507, USA*

The shuttling of polysulfide ions between the electrodes in a lithium-sulfur battery is a major technical issue limiting the self-discharge and cycle life of this high-energy rechargeable battery. Although there have been attempts to suppress the shuttling process, there has not been a direct measurement of the rate of shuttling. We report here a simple and direct measurement of the rate of the shuttling (that we term "shuttle current"), applicable to the study of any type of lithium-sulfur cell. We demonstrate the effectiveness of this measurement technique using cells with and without lithium nitrate (a widely-used shuttle suppressor additive). We present a phenomenological analysis of the shuttling process and simulate the shuttle currents as a function of the state-of-charge of a cell. We also demonstrate how the rate of decay of the shuttle current can be used to predict the capacity fade in a lithium-sulfur cell due to the shuttle process. We expect that this new ability to directly measure shuttle currents will provide greater insight into the performance differences observed with various additives and electrode modifications that are aimed at suppressing the rate of shuttling of polysulfide ions and increasing the cycle life of lithium-sulfur cells.
 [DOI: 10.1149/2.0181501jes]

Manuscript submitted July 21, 2014; revised manuscript received September 26, 2014. Published November 4, 2014. This was Paper 64 presented at the Orlando, Florida, Meeting of the Society, May 11–15, 2014.

The rechargeable lithium-sulfur battery is of great interest due to its high theoretical specific energy of 2600 Wh/kg and also the relatively low cost of sulfur. However, large-scale deployment of lithium-sulfur batteries has been limited by several performance issues relating to power density and cycle life.[1–9] With sulfur at the positive electrode and lithium metal at the negative electrode, the lithium-sulfur battery operates over a voltage range of 1.5 to 2.8 V. The reactions at the positive and negative electrode during charge and discharge are shown schematically in Figure 1. During discharge, sulfur at the positive electrode is reduced progressively to various polysulfides and eventually to the sulfide, while lithium metal at the negative electrode is oxidized to lithium ions. During charge, the lithium ions are reduced to lithium at the negative electrode, and the sulfide is re-oxidized at the positive electrode to the higher-order polysulfides. The organic electrolyte is a 0.5 M solution of lithium bis(trifluoromethanesulfonyl)imide (LiTFSI) in a 1:1 mixture by volume of dioxolane (DOL) and dimethoxyethane (DME). A "solid electrolyte interphase" (SEI) protects the lithium anode from reacting freely with the organic electrolyte. The polysulfides produced during discharge are usually soluble in the battery electrolyte. Lithium-sulfur cells have been the subject of research by several organizations including Sion Power,[10] US Army Research Laboratory[11–13] and more recently by others from Stanford University[14] and Argonne National Laboratory.[15–17] Large cells with a capacity of 2.8 Ah, a practical energy density of 350 Wh/kg and a cycle life of 80 cycles have been demonstrated recently.[10] Smaller coin cells with significantly longer cycle life have also been demonstrated.[14]

Summary of technical challenges with lithium-sulfur batteries.— The principal challenge for the realization of a practical lithium-sulfur battery with long cycle life arises from the solubility of the higher-order polysulfides (S_8^{2-}, S_6^{2-}, S_4^{2-}) in the electrolyte. These polysulfides, generated at the positive electrode during discharge, diffuse to the negative lithium electrode where they are reduced to lower-order polysulfides. The soluble lower-order polysulfides in turn diffuse back to the positive electrode.[18] This shuttling of the polysulfide species results in self-discharge, low round-trip Coulombic efficiency, and irreversible capacity loss. When insoluble sulfides are produced at the negative electrode, these insoluble products cannot diffuse back to the positive electrode, leading to an irreversible capacity loss. Thus, one of the main mechanisms for capacity fade is associated with the shuttling process. Consequently, devising ways to prevent the polysulfide shuttling process through the use of additives,[19] modification of the cathode structure,[20–32] modification of the electrolyte,[33,34] and by other methods[35–37] has been the focus of the recent research efforts in the area of lithium-sulfur batteries.

Quantifying the shuttle process.— Many researchers have explained the shuttle phenomenon in a qualitative manner but there are only a few attempts to quantify the rate of the shuttling process.[18,38,39] Mikhaylik et al have provided a comprehensive discussion of the impact of the polysulfide shuttle process on the self-discharge, charge-discharge efficiency, discharge capacity, and overcharge protection. These researchers have also discussed means of optimizing the cycling conditions based on the shuttle process. A common approach to quantify the shuttle process is the measurement of Coulombic efficiency.[18,19,22,24,25,28–34,40] However, the measured values of Coulombic efficiency can vary considerably with the rate of charge and discharge because of the differences in the duration over which the shuttle process operates. For example, at low rates of charge and discharge, the shuttle operates over a longer period and the impact of the shuttle process on the Coulombic efficiency is high. Similarly, at high rates of charge and discharge, a high value of Coulombic efficiency may be observed; thus, comparison between the results in the literature becomes difficult.

To the best of our knowledge, there has been no direct measurement of the shuttling process or on how the rate of shuttling changes with the state-of-charge. Such a direct measurement of the polysulfide shuttle rates has at least four important benefits:

1. Quantifying the effectiveness of shuttle deterring additives,
2. Assessing the impact of modifications to the cathode structure on the shuttling process
3. Screening for improvements without the need to cycle hundreds of times, and
4. Predicting the effect of the modifications to the shuttle process on cycle life.

Thus, the focus of our study has been to develop a means to directly measure shuttling rates, and to validate the measurement method using practical lithium-sulfur cells.

*Electrochemical Society Active Member.
**Electrochemical Society Fellow.
zE-mail: sri.narayan@usc.edu

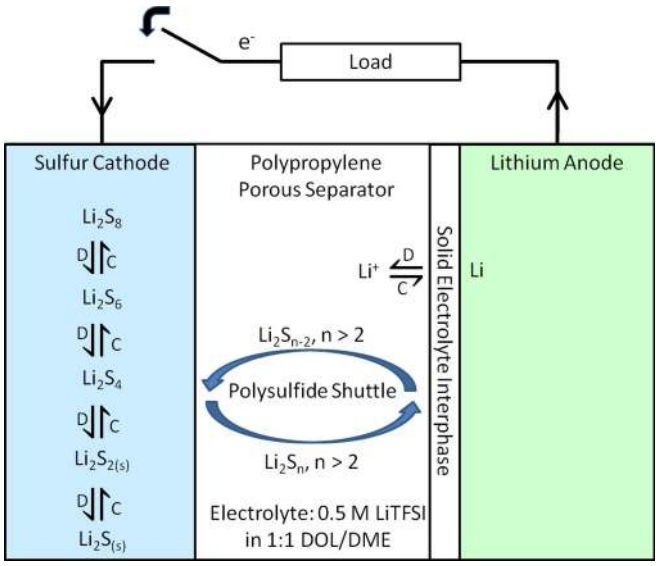

Figure 1. Schematic of the electrochemical processes in a lithium-sulfur battery. C: Charge, D: Discharge.

Phenomenological Basis for the Shuttle Current Measurement

In a lithium-sulfur cell, depending on the state-of-charge, sulfur exists as polysulfides or sulfide of the general formula, Li_2S_n, where n = 1, 2, 4, 6, or 8. In the fully charged state, the polysulfides are of the highest order (n = 8). Upon discharge, the higher-order polysulfides are reduced until the lowest-order polysulfides (n = 1 and 2) are produced. The voltage of a lithium-sulfur cell during discharge ranges from 2.7 to 1.8 V and follows the profile with four distinct regions (Figure 2). Although we start with elemental sulfur in the cathode, in the very first discharge elemental sulfur is reduced to polysulfides (Eq. 1).

$$S_8 + 2Li^+ + 2e^- \rightarrow Li_2S_8 \quad [1]$$

The polysulfides are not usually oxidized completely back to elemental sulfur during charge.[18] At voltages more positive to 2.3 V (Region I of Figure 2), the highest-order polysulfide (n = 8) is reduced to a lower-order polysulfide[41] (n = 6) as per Eq. 2.

$$3Li_2S_8 + 2Li^+ + 2e^- \rightarrow 4Li_2S_6 \quad [2]$$

In the voltage range of 2.3 V to 2.1 V (Region II of Figure 2), the polysulfide with n = 6 is reduced further to soluble products with n = 4 (Eq. 3).

$$2Li_2S_6 + 2Li^+ + 2e^- \rightarrow 3\ Li_2S_4 \quad [3]$$

In the voltage range of 1.9 V to 2.1 V (Region III of Figure 2) the further reduction of the polysulfides to insoluble products (n = 1 and n = 2) occurs as per Eqs. 4 and 5.

$$Li_2S_4 + 2Li^+ + 2e^- \rightarrow 2Li_2S_2\ (\text{insoluble}) \quad [4]$$

$$Li_2S_4 + 6Li^+ + 6e^- \rightarrow 4Li_2S\ (\text{insoluble}) \quad [5]$$

At voltages more negative to 1.9 V (Region III of Figure 2), lithium polysulfide is converted increasingly to insoluble lithium sulfide (Eq. 6).

$$Li_2S_2 + 2Li^+ + 2e^- \rightarrow 2Li_2S\ (\text{insoluble}) \quad [6]$$

The higher-order polysulfides (n > 4, Eqs. 1–3) are soluble in the electrolyte and thus diffuse toward the lithium anode. The potential of the lithium anode being significantly negative to the cathode, allows for further reduction of the polysulfide species. Thus, as further reduction occurs at the anode, the composition and concentration of polysulfides at the anode and cathode become different. This difference in concentration arising from the conversion reactions at the anode generates fluxes of soluble reducible species from the cathode to the anode. Furthermore, the high concentration of reduced species produced at the anode sets up a reverse flux of reduced species from the anode to the cathode. The flux of the reduced species arriving at the cathode from the anode causes the electrode potential of the cathode to become more negative and the cell voltage to decrease. These fluxes of the soluble polysulfide between the anode and the cathode constitute the polysulfide "shuttle".

Under open-circuit conditions, the potential of the anode is relatively constant and is determined by the concentration of lithium ions in the electrolyte and the availability of lithium metal. However, the potential of the cathode decreases steadily because lower-order polysulfides continuously arrive at the cathode from the anode by the shuttling process. However, if we maintained the electrode potential of the cathode at a constant value, then the diffusion fluxes involved in the shuttling process would also maintain a constant value. The electrode potential of the cathode can be maintained by the passage of electric current that will cause re-oxidation of the reduced polysulfides arriving at the cathode. A corresponding reduction reaction will occur at the anode. The applied external current to maintain the cathode potential will equal the diffusional fluxes of the polysulfides in the electrolyte between the cathode and the anode. Thus, by holding the electrode potential or cell voltage constant and measuring the steady-state current through the cell, we can measure the rate of the shuttling process.

The magnitude of the measured shuttle current is dependent on several cell properties:

1. The chosen value of constant electrode potential will determine the concentration of polysulfide species at the cathode, the concentration gradients and consequently, the shuttle current. Therefore, the shuttle current will change with the state-of-charge of the cell.
2. The construction of the cathode, the thickness and porosity of the electrodes, and the porosity and tortuosity of the separator will result in changes in the apparent diffusion coefficients of the various species and thus the value of the shuttle current.
3. The amount of electrolyte, the sulfur loading at the cathode, and the utilization of the cathode determines the concentration of polysulfide species in solution and hence the shuttle current.
4. The electrochemically accessible area for the shuttle reactions at the film-covered anode and the kinetics of the reactions also determine the shuttle current.
5. The retention of the insoluble products of the reduction of soluble polysulfide will cause the shuttle current to decrease in time. Thus,

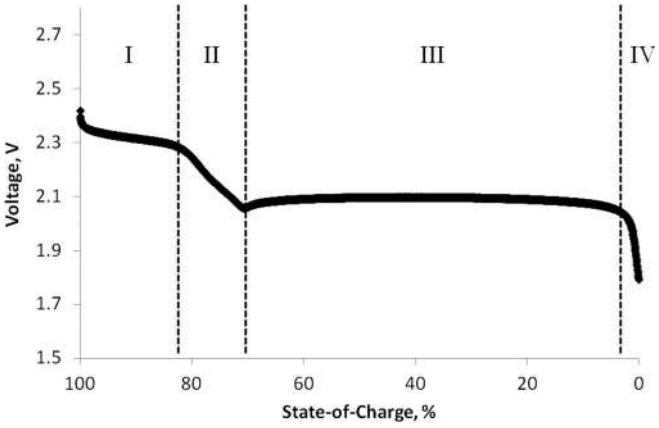

Figure 2. Voltage of a lithium-sulfur cell during discharge at C/20. The redox couples present in each region are as follows, I: Li_2S_8/Li_2S_6, II: Li_2S_6/Li_2S_4, III: Li_2S_4/Li_2S_2, IV: Li_2S_2/Li_2S.

the decrease of shuttle current with time becomes an indicator of the ensuing capacity fade.

Thus, measuring the shuttle current and observing its change in time will offer valuable insights into the factors governing the polysulfide shuttle process in the lithium-sulfur cell. In the subsequent sections we offer a detailed description of the experimental technique for the measurement of the shuttle current and analysis of the experimental results.

Experimental

Cathode fabrication.— Sulfur (Aldrich, 99.5% purity), acetylene black (Alfa Aesar) and polyvinylidene fluoride (PVDF) binder (MTI) were ground in a ball mill. N-methyl-2-pyrrolidone (Aldrich) was added to the mixture to create a slurry that consisted of sulfur (60 wt%), acetylene black (30 wt%), and PVDF (10 wt%). The slurry was coated onto an aluminum foil current collector with a doctor blade. The cathode thickness was approximately 175 micrometers. The coated foil was dried under vacuum for 8 hours at 100°C and then punched into 14 mm diameter disks. The sulfur loading on these disks was approximately 2.7 mg/cm^2.

Cell fabrication.— Coin cells of the 2032-type with aluminum-clad cans (MTI) were assembled using lithium foil (MTI) as the anode, two polypropylene separators (Celgard 2400) and electrolyte consisting of 0.5 M lithium bis(trifluoromethanesulfonyl) imide (LiTFSI, Aldrich) in 1:1 (by volume) dioxolane/dimethyoxethane (Aldrich). Each cell had an electrolyte volume of 140 μL. Cells with 0.5 M LiTFSI that included 0.25 M lithium nitrate (Aldrich) as an additive were also assembled and tested for comparison.

Shuttle current measurements.— At first, the cells were charged and discharged three times at C/20 rate (VersaStat MC potentiostat) to ensure complete "formation" of the cathode. The cells were then charged to 2.7 V and allowed to rest at open circuit for 10 minutes. Following this, the cells were held at the measured value of open circuit voltage and the current applied to the cell was observed for at least 1 to 2 hours during which the current reached a steady-state value. This steady-state current was recorded as the shuttle current. Subsequent shuttle current measurements were conducted by discharging the cell to a target depth-of-discharge (DoD), allowing the cell to equilibrate to an open circuit cell voltage, and then holding the cell voltage at the chosen value and recording the steady-state current as previously described. When the cell was in the fully charged state, a steady current was not observed due to steep changes in concentration resulting from the changes in potential close to 100% state-of-charge in Figure 2. Steady-state currents were observed below 99% state-of-charge up until approximately 75%, the capacity interval wherein the soluble polysulfide species are present.

Results and Discussion

The voltage profile during a typical shuttle current measurement (Figure 3) had distinct sections: (a) the voltage at the end of discharge to the target DoD (b) the voltage relaxation associated with the equilibration of the concentration profile following the removal of the discharge current (c) the voltage at the completion of equilibration and (d) the constant voltage during the shuttle current measurement. After the cell voltage was held constant, the currents increased and approached a steady-state value (Figure 4). In the soluble region, these steady-state currents are directly attributable to the shuttle currents. In the two-phase region where the insoluble products are formed, the shuttle current cannot be measured because the cell voltage does not change with composition. However, insoluble materials do not shuttle and hence the shuttle current will reduce to zero as we move from the soluble region to the insoluble region.

The initial transient in current was due to a small difference between the open-circuit cell voltage and the hold voltage. The negative

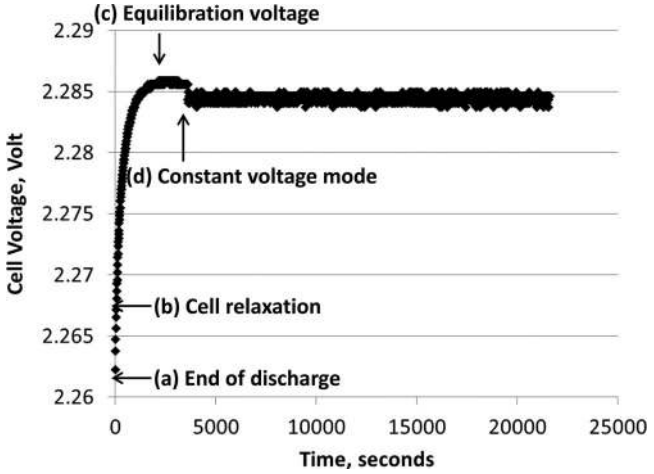

Figure 3. Voltage profile prior to and during shuttle current measurements on lithium-sulfur cell.

current corresponded to the reduction of polysulfide species at the cathode. This reduction current decreased as the internal concentrations adjusted to the chosen fixed value of cell voltage. The positive current observed subsequently is associated with the oxidation of the polysulfide species (such as S_4^{2-} and S_6^{2-}) at the cathode needed to maintain the flux due to the shuttle process. The steady-state current is equal to the steady rate of oxidation of soluble polysulfide species required to maintain the concentration at the cathode at the chosen voltage.

Since the concentration of the various polysulfide species at the cathode varies with the hold voltage, the shuttle current is also expected to change with the state-of-charge of the cell (Figure 5). As the state-of-charge decreased, the shuttle current was found to decrease to almost zero. This trend is to be expected since insoluble polysulfide species are produced as the cell is discharged, and these insoluble products do not shuttle. From Figure 2, it is clear that when we pass from region II to region III, the soluble polysulfide species (S_8^{2-}, S_6^{2-} and S_4^{2-}) become the more insoluble S_2^{2-} species (Eqs. 4, 5). Consistent with this transformation, the shuttle current also drops to a very low value at about 75% state-of-charge (Figure 5). This steady decrease of the shuttle current as more insoluble species are formed, confirmed indirectly that we were measuring the current due to the shuttling of the soluble polysulfide species.

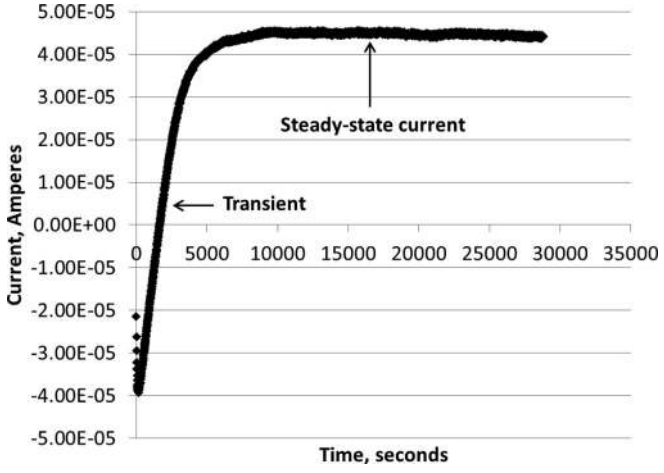

Figure 4. Current profile observed when a cell is held at a constant potential of 2.284 V.

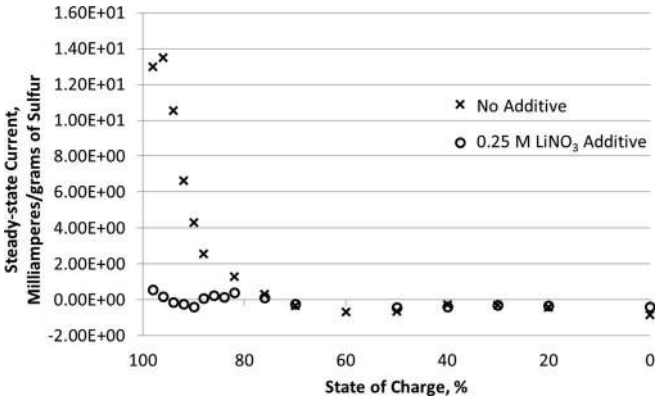

Figure 5: Steady-state current measurements at different states of charge. Steady-state currents above 75% state of charge are directly attributable to shuttle currents. Shuttle currents are normalized to mass of sulfur in the cell.

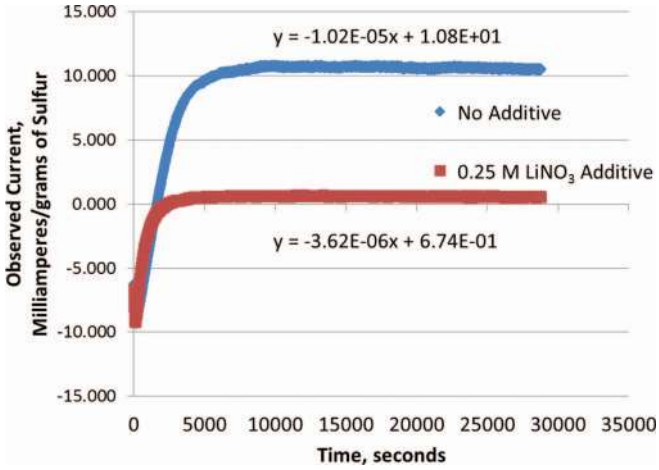

Figure 6: Observed current during potential hold at 95% state of charge for cells with and without lithium nitrate additive. Shuttle current decay rates are calculated after steady-state current is achieved for a lithium-sulfur cell. The algebraic equations express the decay rate.

By the proposed technique, the steady-state currents measured below 75% state-of-charge are not attributable to shuttle currents. In this region (region III of Figure 2), where two separate phases are in equilibrium, the electrode potential is independent of state-of-charge. Consequently, the activities of the polysulfide species in the cell will continue to change but an external current will not be observed since there is no change in voltage. Although the shuttle currents cannot be measured in region III, the shuttle currents do decrease as we approach very low values as we move from region II to region III consistent with the progressive formation of insoluble products (Figure 5).

Lithium nitrate has been demonstrated by other researchers to be effective in suppressing the polysulfide shuttle.[42] In our direct measurement of the shuttle current with 0.25 M lithium nitrate added to the electrolyte, we found that in the region where soluble polysulfide species are expected to be present, the shuttle current dropped to significantly lower values compared to the cell without the additive (Figure 5). The shuttle currents for cells with lithium nitrate additive were almost zero, below 90% state-of-charge. Thus, by this measurement, we have a direct confirmation of the effectiveness of lithium nitrate on suppressing the shuttling process. Lithium nitrate is reduced on the lithium metal surface to form a stable passivation film.[43,44] Specifically, lithium nitrate is reduced on the lithium metal to form Li_xNO_y. Lithium nitrate could also oxidize sulfur species in solution to form Li_xSO_y surface moieties.[45] Our observations of effective suppression of the shuttle currents suggests that the reduction of the polysulfide species at the lithium anode is blocked. This observation is consistent with the formation of a protective film on the anode by lithium nitrate. This film is most likely a surface layer that is electronically-insulating but lithium-ion conducting. Such a surface layer would prevent the irreversible reduction of polysulfide species to insoluble Li_2S_2 and Li_2S while still allowing transport of lithium ions.[45] The lower shuttle current that we observe also means that a substantially lower amount of polysulfide species is being converted to the insoluble lower-order polysulfides at the anode. As stated earlier, prevention of insoluble species at the anode will eliminate the fade of cell capacity due to the shuttle mechanism. The observation of lower shuttle current is consistent with the reports of longer cycle life with lithium-sulfur cells containing lithium nitrate as an electrolyte additive.[42] Cycling studies on coin cells made in our laboratory with lithium nitrate also support this observation of longer cycle life (these results have been provided in the supplementary information section as Item 1). The slight capacity fade for cells with $LiNO_3$ suggests that other modes of degradation are prevailing in cells containing lithium nitrate. However, the shuttle current measurements do confirm that there is little to no capacity fade due to the shuttle mechanism.

We observed slightly negative shuttle current values in the voltage range corresponding to the beginning of formation of the insoluble products (Figure 5). These currents arise from reduction of polysulfide species. It is known that the insoluble lower-order polysulfides such as S_2^{2-} can disproportionate[46] to a small extent to produce some higher-order soluble polysulfides S_4^{2-} as per Eq. 7.

$$3S_2^{2-} \rightleftharpoons S_4^{2-} + 2S^{2-} \quad [7]$$

This disproportionation reaction increases the concentration of S_4^{2-} at the cathode causing the electrode potential to become more positive and requiring reduction currents to return these species back to S_2^{2-} to maintain the concentrations consistent with the hold voltage. This type of disproportionation behavior is also consistent with the shape of the cell voltage profile during discharge where a slight dip is observed in the region of corresponding to 50–75% state-of-charge (Figure 2).

We also found that although a steady-state shuttle current was maintained over long periods (one to two hours), there was a very slow decrease of the shuttle current when the observations were continued over a ten-hour period (Figure 6). This decrease of the shuttle current albeit small, does suggest that the concentration gradients do change over time. One factor that will cause this type of decrease in shuttle current is the formation of insoluble polysulfides at the anode. As insoluble products are produced, the concentration of soluble materials is slowly reduced and consequently the shuttle current also decreases. If this is indeed the underlying process for the decrease of shuttle current, we can relate the rate of decrease of shuttle current to the rate of formation of insoluble products and also the irreversible capacity fade caused by the formation of these insoluble products.

The results of the long-duration shuttle current measurements at 95% state-of-charge for a lithium-sulfur cell with and without the lithium nitrate are shown in Figure 6. We found that the rate of decrease of shuttle current was almost an order of magnitude lower in the presence of the lithium nitrate additive. These observations suggested that the concentration gradients changed at a lower rate in the presence of the additive and less of the insoluble products were generated at the anode. These observations were also consistent with the beneficial effect of the lithium nitrate additive on the cycle life of the lithium-sulfur cell.

Analysis of shuttle currents.— In the following, we present a simple one-dimensional phenomenological model of the polysulfide shuttle process to understand and simulate the experimental results of the steady-state shuttle current measurements. We also show how the slow decrease of shuttle current with time at any particular state-of-charge relates to the capacity fade due to the polysulfide shuttle process. For the analysis we assume the following:

1. Only the soluble polysulfide species (S_8^{2-}, S_6^{2-} and S_4^{2-}) participate in the shuttling process.

2. The electrode potential at the lithium anode is sufficiently negative to completely convert S_8^{2-} and S_6^{2-} to S_4^{2-}.
3. The conversion of S_4^{2-} at the anode to insoluble materials (Li_2S_2 and Li_2S) is a relatively slow process compared to the interconversion of the soluble polysulfides. This process is anywhere from 100 to 3000 times slower depending on the state of charge and activities of polysulfide species present. (Supporting calculations are provided in the supplementary information section as Item 3.)

During the shuttling of polysulfide species, the concentrations of the redox species vary across the width of the cell. At the cathode, the concentrations of these species are determined by the electrode potential and the reversible electrochemical equilibrium between the redox species. At the anode, the soluble polysulfide species is entirely S_4^{2-} because of the relatively negative electrode potential of the lithium electrode.

While the polysulfides S_8^{2-}, S_6^{2-} and S_4^{2-} are soluble in the electrolyte, Li_2S_2 and Li_2S are relatively insoluble and will remain within the body of the positive electrode. Specifically, the concentration of soluble polysulfides (S_8^{2-}, S_6^{2-} and S_4^{2-}) during cell operation is expected in the range of 0.1–0.2 M based on the sulfur loading at the cathode (see supporting calculation in the supplementary section as Item 2). This concentration is well below the solubility limits for these polysulfides. The equilibrium electrode potential of the cathode at various states of charge is determined by the Nernst equation. In the regions I and II (Figure 2), the equilibrium electrode potentials are given by,

$$E = E_I^{o'} + \frac{RT}{2F}\ln\frac{\left[S_8^{2-}\right]^3}{\left[S_6^{2-}\right]^4} \quad [8]$$

$$E = E_{II}^{o'} + \frac{RT}{2F}\ln\frac{\left[S_6^{2-}\right]^2}{\left[S_4^{2-}\right]^3} \quad [9]$$

where $E_I^{o'}$ and $E_{II}^{o'}$ are the formal reduction potentials for the S_8^{2-}/S_6^{2-} and S_6^{2-}/S_4^{2-} couple, respectively. The values of $E_I^{o'}$ and $E_{II}^{o'}$ were estimated from the discharge curve in Figure 2 to be 2.32 V and 2.22 V vs. the Li^+/Li electrode, respectively.

All the soluble sulfur species originates from the elemental sulfur loading at the positive electrode. For N moles of sulfur (S_8) present at the positive electrode, and for a utilization fraction U, NU is the number of moles of S_8 found in the soluble region of the discharge curve, distributed among S_8^{2-}, S_6^{2-} and S_4^{2-}. In the absence of the shuttle process, these concentrations will stay uniform throughout the cell. If A is the cross-sectional area of the cell, and δ is the inter-electrode distance, then the total amount of sulfur in the soluble form, in the absence of the shuttle process, can be related to the uniform concentration of the three soluble polysulfides by Eq. 10.

$$(NU/A\delta) = [C_{S8} + (3/4)C_{S6} + (1/2)C_{S4}] \quad [10]$$

where C_{S8} is the concentration of S_8^{2-}, C_{S6} is the concentration of S_6^{2-}, and C_{S4} is the concentration of S_4^{2-}, A is the area of the electrode, δ is the inter-electrode distance, and U is the utilization fraction for the sulfur electrode. The factor 3/4 arises from each mole of S_8^{2-} reacting to produce 4/3 moles of S_6^{2-}, and similarly the factor 1/2 arises from each mole of S_8^{2-} reacting to produce 2 moles of S_4^{2-} at the sulfur electrode (Eqs. 2, 3). The concentration between the three soluble species will vary with the state-of-charge of the cell.

When the polysulfide species undergo reaction at the anode, and when the shuttle process occurs, the concentrations will not be uniform although the total number of moles of sulfur will still be the same. When the shuttle process is operating, the steady-state concentrations of the various soluble forms of the polysulfide species will change in a linear manner between the two electrodes as per Fick's first law. For a chosen value of electrode potential at the cathode, we can determine these concentration gradients between the cathode and the anode. In the steady-state, when linear concentration gradients are established between the electrodes we can compute the total amount of soluble sulfur species as per Eq. 11.

$$NU/A\delta = (1/2)[(C_{S8,c} - C_{S8,a}) + (3/4)(C_{S6,c} - C_{S6,a}) + (1/2)(C_{S4,c} + C_{S4,a})] \quad [11]$$

The subscripts "c" and "a" refer to the cathode and anode. The electrode potential of the lithium anode being sufficiently negative, we can expect the concentration of S_8^{2-} and S_6^{2-} to be zero and consequently we may assign $C_{S8,a} = 0$ and $C_{S6,a} = 0$ in Eq. 11 to yield Eq. 12.

$$(NU/A\delta) = [(1/2)C_{S8,c} - (3/8)C_{S6,c} + (1/4)C_{S4,c} + (1/4)C_{S4,a}] \quad [12]$$

Since the electrode potential of the sulfur cathode is maintained at a constant value during the shuttle current measurement, the surface concentrations, $C_{S8,c}$, $C_{S6,c}$ and $C_{S4,c}$ are also constant as defined by the corresponding Nernst equations (Eqs. 8, 9). However, to maintain this electrode potential, a current must flow through the electrode to counteract the diffusion fluxes that arise from the three concentration gradients (Eqs. 13–15).

$$\text{Diffusion flux of } S_8^{2-} = A\, D_{S8}\, C_{S8,c}/\delta \quad [13]$$

$$\text{Diffusion flux of } S_6^{2-} = A\, D_{S6}\, C_{S6,c}/\delta \quad [14]$$

$$\text{Diffusion flux of } S_4^{2-} = A\, D_{S4}\, (C_{S4,a} - C_{S4,c})/\delta \quad [15]$$

D_{S8}, D_{S6} and D_{S4} are the apparent diffusion coefficients for S_8^{2-}, S_6^{2-} and S_4^{2-}, respectively. While there is likely to be a difference in the value of the apparent diffusion coefficients within the electrolyte and the electrode structure, we do not differentiate this in this first-order, simplified analysis.

In the steady-state, the diffusional fluxes of S_8^{2-} and S_6^{2-} from the cathode to the anode must be balanced by the flux of S_4^{2-} from the anode to the cathode. Since the mole equivalents for S_8^{2-}, S_6^{2-}, and S_4^{2-} are in the ratio of 1: 3/4 : 1/2, the molar fluxes are expected to balance out in the same ratio as per Eq. 16.

$$(D_{S8}C_{S8,c}) + (3/4)(D_{S6}C_{S6,c}) = (1/2)D_{S4}(C_{S4,a} - C_{S4,c}) \quad [16]$$

An external current, I, equal to these diffusion fluxes (Eq. 16) must be applied to maintain the concentration at the cathode and the steady-state concentration gradients across the cell. Therefore, we term I as the shuttle current and relate this current to the concentration gradients (Eq. 17a and 17b).

$$I = 2F\, A\, K[(D_{S8}C_{S8,c}) + (3/4)(D_{S6}C_{S6,c})]/\delta \quad [17a]$$

$$\text{And} \quad I = 2F\, A\, K(1/2)D_{S4}(C_{S4,a} - C_{S4,c})/\delta \quad [17b]$$

where F is the faraday constant, A is the area of the electrode and K is permeability of the film-covered anode to polysulfide reactions.

Upon determination of the values of $C_{S8,c}$ and $C_{S6,c}$ (from Eqs. 8, 9, 12, 13), the external current I, equal in magnitude to the shuttle current, can be calculated from Eq. 17a. In this manner, we can also determine the magnitude of the shuttle current and its dependency on the state-of-charge of the cell.

Model verification.— To verify our simple one-dimensional model of the shuttling process we have used Eqs. 8–17 to simulate the dependency of shuttle current on the state-of-charge and have compared this with the experimental results (Figure 7). Such a simulation was performed with the following values: $E_I^{o'} = 2.32$ V, $E_{II}^{o'} = 2.22$ V, $D_{S8} = 6 \times 10^{-7}$ cm^2 s^{-1}, $D_{S6} = 6 \times 10^{-7}$ cm^2 s^{-1}, $D_{S4} = 1 \times 10^{-7}$ cm^2 s^{-1}, $\delta = 0.0225$ cm, $N = 1.6418 \times 10^{-5}$ mol cm^{-3}, $A = 1.53$ cm^2, $K = 0.1$, $U = 49.5\%$ at room temperature.

The values of the various parameters used in the simulation were experimentally accessible parameters for the specific cell for which we intended to verify the model results. The values of $E_I^{o'}$ and $E_{II}^{o'}$ were estimated from the discharge curve (Figure 2) and Eqs. 8 and 9. In Figure 2, for region I, the $E_I^{o'}$ value for corresponded to the cell voltage when the molar ratio is 3:4 for S_8^{2-}:S_6^{2-}, or when 3/7th of the

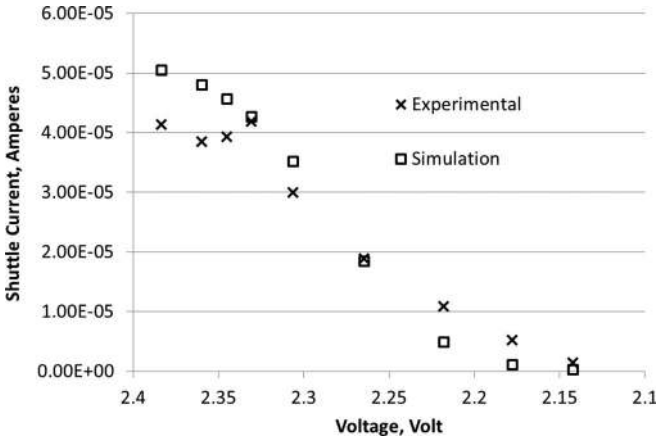

Figure 7. Comparison of simulation and experimental results of shuttle current at various values of cell voltage. Experimental data is the same as in Figure 5 for the cell with no additive.

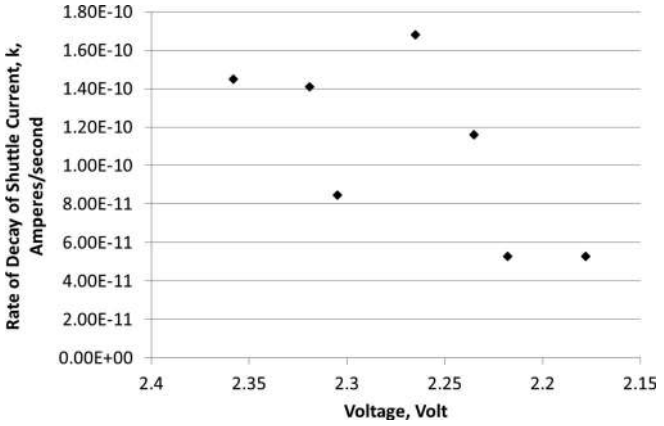

Figure 8. The rate of decrease of shuttle current at various values of cell voltage.

capacity in region I was discharged. Similarly, $E_{II}^{o'}$ was determined from region II at a molar ratio of 2:3 for S_6^{2-}:S_4^{2-} or when 2/5th of the capacity in region II was discharged.

The diffusion coefficients were based on the solution value of 6 $\times 10^{-6}$ cm^2 s^{-1} for S_8^{2-} and S_6^{2-} and 1 $\times 10^{-6}$ cm^2 s^{-1} for S_4^{2-}.[47] This value of diffusion coefficient in free electrolyte was decreased by one order of magnitude to account for the tortuosity and porosity of the two Celgard polypropylene separators to obtain an apparent value of the diffusion coefficient; the porosity of each separator layer being about 55%, leads to a net porosity of 30%; a tortuosity factor of 3 is appropriate for the Celgard separator. Based on these corrections, the apparent diffusion coefficient in the cell was estimated to be 6 $\times 10^{-7}$ cm^2 s^{-1} for S_8^{2-} and S_6^{2-} and 1 $\times 10^{-7}$ cm^2 s^{-1} for S_4^{2-}. The permeability of the lithium-ion conducting and electronically insulating anode film was estimated to be 10%.

The utilization fraction, U, was calculated from the experimental value of initial discharge capacity of the cell and the loading of sulfur in the cathode. The total number of moles of S_8^{2-} and N, were calculated from the sulfur loading at the cathode. The inter-electrode distance, δ, was calculated by summing the thickness of the cathode and two separators used.

The simulated shuttle current based on this set of realistic values of input properties of the cell matches that of the experimentally measured shuttle current as a function of state-of-charge quite well (Figure 7). Such a close agreement between the experimental results and mathematical simulation over the entire range of cell voltage suggested that we have a valid phenomenological description of the soluble polysulfide shuttling between the electrodes, and also that the experimental value of applied current actually corresponded to the shuttling process.

Predicting capacity fade.— In our measurement of the steady-state shuttle current, we notice a slow decay of this current value over several hours. This decay in our view is not any experimental artifact, but an indication of the changes in concentration gradients that are caused by partial reduction of the products at the anode to insoluble lithium polysulfide (Li_2S_2) and lithium sulfide (Li_2S). As stated earlier, the formation of such insoluble products will result in loss of the discharge capacity over multiple cycles. If this was indeed the case, then the measurement of the rate of decay of shuttle current would enable us to estimate number of cycles during which a certain fraction of the cathode capacity would be lost. The decay of shuttle current with time will reflect the irreversible sequestration of insoluble sulfur species at the anode and also at the cathode.

From the results presented in Figure 6 it appeared that the shuttle current decreased linearly with time. From Eq. 17b, we may relate the rate of change in shuttle current, $\Delta I/\Delta t$, or the slope of the decay curve, k, to the concentration gradients using Eq. 18.

$$(\Delta I)/(\Delta t) = k = 2F\ A\ K(1/2)D_{S4}(C_{S4,al} - C_{S4,a2})/[\delta(\Delta t)] \quad [18]$$

Where $\Delta t = t_2 - t_1$, $C_{S4,a1}$ and $C_{S4,a2}$ are the concentrations of S_4^{2-} at the anode at times t_1 and t_2, respectively.

Experimental studies on the rate of decay of the shuttle current indicate that the slope value k varies with the cell voltage (Figure 8). Let us consider an average value of k, namely k_{avg}, to simplify the rest of the analysis. Then, Eqn. 18 can be rearranged to obtain the rate of change in concentration of S_4^{2-} at the anode with time.

$$(C_{S4,al} - C_{S4,a2})/\Delta t = (k_{avg}\delta)/(F\ A\ K\ D_{S4}) \quad [19]$$

Since the change in the concentration of S_4^{2-} at the anode results from the formation of insoluble products, we can relate the rate of conversion of S_4^{2-} to the formation of the rate of formation of insoluble and non-cycleable products,

$$(C_{S4,a1} - C_{S4,a2})(A\delta)/(\Delta t) = (k_{avg}\delta^2)/(2F\ A\ K\ D_{S4}) \quad [20]$$

As per Eq. 21, each mole of S_4^{2-} originates from 0.5 mole of S_8^{2-}.

$$0.5\,S_8^{2-} + 2e^- \rightleftharpoons S_4^{2-} + 4e^- \rightleftharpoons S_2^{2-} + 2S^{2-} \quad [21]$$

Therefore, 6 Faradays of cell capacity is lost for every 0.5 mole of S_8^{2-} that is lost to insoluble products. Q_{irr}, the total capacity lost irreversibly by the reduction of S_4^{2-} to insoluble products at the anode over the period Δt, is then given by,

$$Q_{irr} = (3/2)k_{avg}(\Delta t)\delta^2/(K(1/2)D_{S4}) \quad [22]$$

If during every cycle, the cell stays in the region where soluble polysulfides are present (Region I and II of Figure 2) for a total time of Δt, then Q_{irr} will be the capacity lost in each cycle. If Q^o was the discharge capacity of the cell in the first cycle then the number of cycles, N_{cycles}, over which the cell loses 20% of its initial capacity is given by

$$N_{cycles} = 0.8\left(Q^0/Q_{irr}\right) \quad [23]$$

Or substituting from Eq. 22,

$$N_{cycles} = 0.8Q^0(K/(1/2)D_{S4})/\left[(3/2)k_{avg}(\Delta t)\delta^2\right] \quad [24]$$

Thus, in Eq. 24 we have an expression relating the cycle life to the rate of decay shuttle current.

We have substituted in Eq. 24 the values for the various properties from experimental measurements on cells without lithium nitrate additive. The property values used in this calculation are: $Q^o = 12.42$ C, $k_{avg} = 1.09 \times 10^{-10}$ A s^{-1}, K = 0.1, $\Delta t = 15600$ s, $\delta = 2.25 \times 10^{-2}$ cm, $D_{S4} = 1 \times 10^{-7}$ cm^2 s^{-1}. The value of 15600 seconds is obtained from doubling the time of 7800 seconds that the cell stays in the region where soluble polysulfides are present during discharge at C/20 rate. The value of N_{cycles} for the cell to reach 80% of its initial capacity

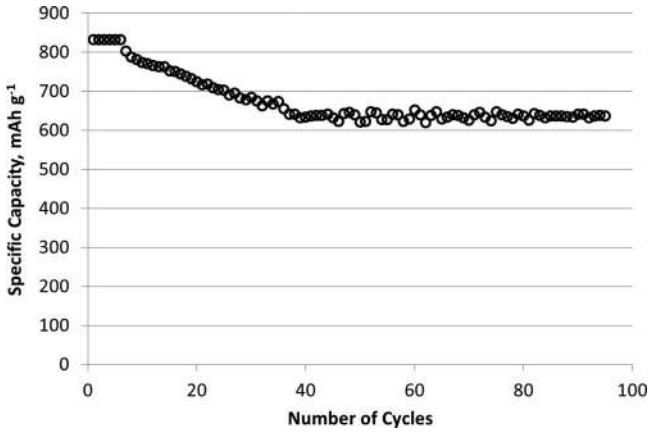

Figure 9. Capacity fade of lithium-sulfur cell without additives cycled at C/20.

based on the foregoing properties is calculated to be approximately 39 cycles. From our experimental studies of cycling of lithium-sulfur cells (Figure 9) we find that after 39 cycles, a lithium-sulfur cell without additives retained 76% of the capacity. This value of capacity retention is quite close to the 80% value predicted from Eq. 24. For the range of k values observed, the variation in the number of cycles predicted spans just a few tens of cycles. At least a couple of orders of magnitude change in k value is needed before a substantial change in cycle life can be observed.

Thus, the rate of decay of shuttle current with time can be used to predict the cycle life of cells where the mechanism of loss is due to the formation of insoluble products at the anode. Improvements that inhibit the formation of insoluble products should result in longer cycle life. Since the prediction of capacity loss is based on the formation of insoluble products at the anode, other mechanisms that contribute to capacity fade are not considered here. The foregoing analysis also assumes that factors and mechanisms that govern the shuttle current will remain in effect through the entire duration of cycle life of the cell. In the case of cells with the lithium nitrate additive, lithium nitrate is consumed over time.[43–45] Consequently, after all of the lithium nitrate is consumed, the shuttle current could change dramatically, and this point in the life of the cell may be monitored by the shuttle current measurements.

Conclusions

We have demonstrated a simple and effective technique of directly measuring polysulfide shuttle currents in lithium-sulfur batteries. We have analyzed the results of these experimental measurements of the shuttle current using a simplified one-dimensional phenomenological model. The simulation results based on this model match well with the experimental results, validating our understanding of the shuttle current measurements. From the decay of shuttle currents with time, we have a shown a way to predict the cycle life of the lithium-sulfur cell. Thus, shuttle current measurements can be used in place of cycling a cell multiple times to determine especially the effectiveness of shuttle suppressing additives, electrode modifications, and other methods of deterring the polysulfide shuttle. We expect these shuttle current measurements to be useful in screening particularly shuttle deterrents and also rationalizing the cycle life improvements obtained with electrode and electrolyte modifications.

Acknowledgment

The research reported here was supported by the Loker Hydrocarbon Research Institute, University of Southern California, and the U.S. Department of Energy - PIP Program for financial support to Derek Moy during the summer semester of 2013.

References

1. J. R. Akridge, Y. V. Mikhaylik, and N. White, *Solid State Ionics*, **175**(1–4), 243 (2004).
2. B. L. Ellis, K. T. Lee, and L. F. Nazar, *Chemistry of Materials*, **22**(3), 691 (2010).
3. B. Scrosati and J. Garche, *Journal of Power Sources*, **195**(9), 2419 (2010).
4. M.-K. Song, E. J. Cairns, and Y. Zhang, *Nanoscale*, **5**(6), 2186 (2013).
5. M. Barghamadi, A. Kapoor, and C. Wen, *Journal of the Electrochemical Society*, **160**(8), A1256 (2013).
6. S. S. Zhang, *Journal of Power Sources*, **231**, 153 (2013).
7. R. Xu, I. Belharouak, X. Zhang, B. Polzin, and J. C. M. Li, in *Energy Harvesting and Storage: Materials, Devices, and Applications Iv*, N. K. Dhar, P. Balaya, and A. K. Dutta, eds., Vol. 8728 (2013).
8. Y.-X. Yin, S. Xin, Y.-G. Guo, and L.-J. Wan, *Angewandte Chemie-International Edition*, **52**(50), 13186 (2013).
9. L. F. Nazar, M. Cuisinier, and Q. Pang, *MRS Bulletin*, **39**(5), 436 (2014).
10. Y. Mikhaylik, I. Kovalev, R. Schock, K. Kumaresan, J. Xu, and J. Affinito, *Battery/Energy Technology (General) - 216th ECS Meeting*, **25**(35), 23 (2010).
11. S. S. Zhang, *Journal of the Electrochemical Society*, **159**(8), A1226 (2012).
12. S. S. Zhang, *Energies*, **5**(12), 5190 (2012).
13. S. S. Zhang and D. T. Tran, *Journal of Materials Chemistry A*, **2**(20), 7383 (2014).
14. Z. W. Seh, W. Li, J. J. Cha, G. Zheng, Y. Yang, M. T. McDowell, P.-C. Hsu, and Y. Cui, *Nature Communications*, **4** (2013).
15. W. Weng, V. G. Pol, and K. Amine, *Advanced Materials*, **25**(11), 1608 (2013).
16. R. Xu, I. Belharouak, J. C. M. Li, X. Zhang, I. Bloom, and J. Bareno, *Advanced Energy Materials*, **3**(7), 833 (2013).
17. R. Chen, T. Zhao, J. Lu, F. Wu, L. Li, J. Chen, G. Tan, Y. Ye, and K. Amine, *Nano Letters*, **13**(10), 4642 (2013).
18. Y. V. Mikhaylik and J. R. Akridge, *Journal of the Electrochemical Society*, **151**(11), A1969 (2004).
19. Z. Lin, Z. Liu, W. Fu, N. J. Dudney, and C. Liang, *Advanced Functional Materials*, **23**(8), 1064 (2013).
20. G. He, X. Ji, and L. Nazar, *Energy & Environmental Science*, **4**(8), 2878 (2011).
21. H. Wang, Y. Yang, Y. Liang, J. T. Robinson, Y. Li, A. Jackson, Y. Cui, and H. Dai, *Nano Letters*, **11**(7), 2644 (2011).
22. J. Guo, Y. Xu, and C. Wang, *Nano Letters*, **11**(10), 4288 (2011).
23. H. Schneider, A. Garsuch, A. Panchenko, O. Gronwald, N. Janssen, and P. Novak, *Journal of Power Sources*, **205** 420 (2012).
24. N. Li, M. Zheng, H. Lu, Z. Hu, C. Shen, X. Chang, G. Ji, J. Cao, and Y. Shi, *Chemical Communications*, **48**(34), 4106 (2012).
25. Z. Deng, Z. Zhang, Y. Lai, J. Liu, Y. Liu, and J. Li, *Solid State Ionics*, **238**, 44 (2013).
26. Y.-S. Su and A. Manthiram, *Electrochimica Acta*, **77**, 272 (2012).
27. B. Ding, C. Yuan, L. Shen, G. Xu, P. Nie, Q. Lai, and X. Zhang, *Journal of Materials Chemistry A*, **1**(4), 1096 (2013).
28. J. Guo, Z. Yang, Y. Yu, H. D. Abruna, and L. A. Archer, *Journal of the American Chemical Society*, **135**(2), 763 (2013).
29. M. He, L.-X. Yuan, W.-X. Zhang, and Y.-H. Huang, *Journal of Solid State Electrochemistry*, **17**(6), 1641 (2013).
30. J.-Q. Huang, Q. Zhang, S.-M. Zhang, X.-F. Liu, W. Zhu, W.-Z. Qian, and F. Wei, *Carbon*, **58**, 99 (2013).
31. H. Chen, W. Dong, J. Ge, C. Wang, X. Wu, W. Lu, and L. Chen, *Scientific Reports*, **3** (2013).
32. B. Ding, L. Shen, G. Xu, P. Nie, and X. Zhang, *Electrochimica Acta*, **107**, 78 (2013).
33. L. Suo, Y.-S. Hu, H. Li, M. Armand, and L. Chen, *Nature Communications*, **4** (2013).
34. L. Wang and H. R. Byon, *Journal of Power Sources*, **236**, 207 (2013).
35. A. Manthiram, Y. Fu, and Y.-S. Su, *Accounts of Chemical Research*, **46**(5), 1125 (2013).
36. Y. Yang, G. Zheng, and Y. Cui, *Energy & Environmental Science*, **6**(5), 1552 (2013).
37. S. R. Chen, F. Dai, M. L. Gordin, and D. H. Wang, *Rsc Advances*, **3**(11), 3540 (2013).
38. A. F. Hofmann, D. N. Fronczek, and W. G. Bessler, *Journal of Power Sources*, **259**, 300 (2014).
39. M. R. Busche, P. Adelhelm, H. Sommer, H. Schneider, K. Leitner, and J. Janek, *Journal of Power Sources*, **259**, 289 (2014).
40. Y.-S. Su and A. Manthiram, *Nature Communications*, **3** (2012).
41. Y. V. Mikhaylik and J. R. Akridge, *Journal of the Electrochemical Society*, **150**(3), A306 (2003).
42. Y. V. Mikhaylik in "U.S. Patent", patent No. 7,553,590 (2009).
43. S. S. Zhang, *Electrochimica Acta*, **70**, 344 (2012).
44. S. S. Zhang, *Electrochimica Acta*, **97**, 226 (2013).
45. D. Aurbach, E. Pollak, R. Elazari, G. Salitra, C. S. Kelley, and J. Affinito, *Journal of the Electrochemical Society*, **156**(8), A694 (2009).
46. V. S. Kolosnitsyn and E. V. Karaseva, *Russian Journal of Electrochemistry*, **44**(5), 506 (2008).
47. K. Kumaresan, Y. Mikhaylik, and R. E. White, *Journal of the Electrochemical Society*, **155**(8), A576 (2008).